

MODELING THE TENUOUS INTRACLUSTER MEDIUM IN GLOBULAR CLUSTERS

J. NAIMAN, M. SOARES-FURTADO, AND E. RAMIREZ-RUIZ¹

Draft April 1, 2022

ABSTRACT

We employ hydrodynamical simulations to investigate the underlying mechanism responsible for the low levels of gas and dust in globular clusters. Our models examine the competing effects of mass supply from the evolved stellar population and energy injection from the main sequence stellar members for globular clusters 47 Tucanae, M15, NGC 6440, and NGC 6752. Disregarding all other gas evacuation processes, we find that the energy output from the main sequence stellar population alone is capable of effectively clearing the evolved stellar ejecta and producing intracluster gas densities consistent with current observational constraints. This result distinguishes a viable ubiquitous gas and dust evacuation mechanism for globular clusters. In addition, we extend our analysis to probe the efficiency of pulsar wind feedback in globular clusters. The detection of intracluster ionized gas in cluster 47 Tucanae allows us to place particularly strict limits on pulsar wind thermalization efficiency, which must be extremely low in the cluster's core in order to be in accordance with the observed density constraints.

1. INTRODUCTION

For over half a century, globular cluster observations have revealed a paucity of intracluster dust and gas. Given the abundance of evolved stellar ejecta and the extensive timescales between galactic disk crossing events, these observations are at odds with theoretical expectations. Orbiting in the Galactic halo, globular clusters traverse through the plane of the galaxy on timescales of 10^8 years, expelling the intracluster medium with each passage (Odenkirchen et al. 1997). Between galactic disk crossing events, the evolving stellar members continuously fill the cluster with stellar ejecta. These stars are about $0.8M_{\odot}$ at the main sequence turn-off and, during the evolution to the white dwarf stage, 10-100 M_{\odot} of material is predicted to have been accumulated (Tayler & Wood 1975). The hunt for this elusive intracluster medium has been extensive, yet the majority of observations have been fruitless. Searches for dust and atomic, molecular, and ionized gas have been carried out, resulting in upper limits and detections that are generally much lower than the values expected if the mass was effectively retained.

Submillimeter and infrared (IR) searches for dust in globular clusters (Lynch & Rossano 1990; Knapp et al. 1995; Origlia et al. 1996; Hopwood et al. 1999) have predominately resulted in low dust mass content upper limits on the order of $\leq 4 \times 10^{-4}M_{\odot}$ (Barmby et al. 2009), as compared to predicted dust masses ranging from $10^{-0.8} - 10^{-3.6}M_{\odot}$. Tentative evidence for excess IR emission from cool dust in the metal-rich globular cluster NGC 6356 was found nearly two decades ago (Hopwood et al. 1998), although the lack of a 90 μm excess casts doubt on this detection (Barmby et al. 2009). Only the Galactic globular cluster M15 (NGC 7078) depicts clear evidence for an IR excess (Evans et al. 2003; Boyer et al. 2006), revealing a cluster dust mass of $9 \pm 2 \times 10^{-4}M_{\odot}$, which is at least one order of magnitude below the predicted value. The lack of intracluster dust might suggest that evolved stars produce less dust than predicted, although evidence to the contrary has been found in M15 and NGC 5139, where some of the dustiest, most mass expelling stars have been found (Boyer et al. 2006, 2008).

Troland et al. (1978) led the first search for 2.6 mm CO emission in globular clusters, which resulted in a non-detection, but lacked sufficient sensitivity to rule out the presence of molecular gas. Since then, upper limits have been placed on the molecular gas content in globular clusters, constraining the mass to about $0.1 M_{\odot}$ (Smith et al. 1995; Leon & Combes 1996). The most promising search lead to a tentative detection of two CO lines in the direction of globular cluster 47 Tucanae (NGC 104), which was interpreted to be the result of the bow shock interaction generated as the cluster traverses through the Galactic halo (Origlia et al. 1997). Other searches, including attempts to measure OH and H₂O maser emission, have been unsuccessful (Knapp & Kerr 1973; Kerr et al. 1976; Frail & Beasley 1994; Cohen & Malkan 1979; Dickey & Malkan 1980; van Loon et al. 2006).

Neutral hydrogen (HI) at 21-cm was detected in NGC 2808, measuring $200M_{\odot}$ of gas (Faulkner et al. 1991). This is not beyond dispute, however, since there is known to be a foreground 21-cm extended region around the cluster. Most other attempts to detect HI in globular clusters have been unsuccessful or resulted in upper limits on the order of a few solar masses (Heiles & Henry 1966; Robinson 1967; Kerr & Knapp 1972; Knapp et al. 1973; Bowers et al. 1979; Birkinshaw et al. 1983; Lynch et al. 1989; Smith et al. 1990; van Loon et al. 2006, 2009). A tentative HI detection of $0.3M_{\odot}$ in M15 was presented by van Loon et al. (2006) using 21-cm Arecibo observations.

The most reliable constraints on the presence of intracluster material have been derived from radio dispersion measurements of known millisecond pulsars in 47 Tucanae (Camilo et al. 2000), which resulted in the first detection of ionized gas with a density of $n_e = 0.067 \pm 0.015 \text{ cm}^{-3}$ (Freire et al. 2001b). This ionized gas measurement, as well

¹ Department of Astronomy and Astrophysics, University of California, Santa Cruz, CA 95064

as the upper limits placed on ionized gas in other clusters (Smith et al. 1976; Faulkner & Freeman 1977; Knapp et al. 1996), correspond to a deficiency of gas by two or three orders of magnitude when compared to the amount predicted by the effective accumulation of evolved stellar ejecta within the observed clusters.

The paucity of intracluster gas hints at the desirability for a common mechanism that acts to constantly remove gas from the cluster. Potential gas evacuation processes may be external or internal to the globular cluster itself. One external process is ram pressure stripping of the intracluster medium as the globular cluster traverses through the surrounding hot galactic halo. This mechanism has been investigated both analytically and numerically in the past. Frank & Gisler (1976) found that the interstellar medium of the Galactic halo was one order of magnitude too low in density to account for the stripping of the cluster. Priestley et al. (2011), aided by the use of three-dimensional hydrodynamical simulations, revisited this problem and concluded that halo sweeping was only an effective gas evacuation mechanism for globular clusters $\leq 10^5 M_\odot$. This is further compounded by the fact that the majority of the globular clusters reside in low density regions of the halo.

Internal evacuation mechanisms are more varied in scope with some being impulsive and others being continuous in nature. Vandenberg & Faulkner (1977) suggested the possibility that UV heating from the horizontal branch (HB) stellar population might provide sufficient energy input to explain the low gas densities in clusters, however not all clusters contain hot HB stars. Umbreit et al. (2008) argues that the energy injected by stellar collisions could be significant, in particular in clusters with high encounter rates. Coleman & Worden (1977) investigated the possibility that flaring M-dwarf stars might supply the energy injection required to evacuate the cluster, however the number and distribution of M-dwarf stars in clusters is highly uncertain. The energy injection from hydrogen rich novae explosions is another possible gas evacuation mechanism, which was investigated early on by Scott & Durisen (1978) and more recently by Moore & Bildsten (2011). However, it is highly uncertain whether these explosions occur with enough frequency (Bode & Evans 2008) and if the beamed structure of the emanating outflows will lead to significantly lower gas removal efficiencies (O'Brien et al. 2006). Finally, the presence of millisecond pulsars in many of these systems not only enables the placement of stringent intracluster density constraints, but also provides globular clusters with yet another mechanism of energy injection (Spergel 1991).

Several mechanisms for gas removal have been discussed above, with internal energy injection processes being favored over ram pressure stripping, however the contribution of the discussed internal processes is expected to vary significantly between clusters such that, individually, they would be unable to explain the universality of low gas densities seen across all globular clusters. Mass and energy injection from stellar winds, on the other hand, are a common feedback ingredient in all clusters. In the past, it has been argued that the evolved stellar ejecta does not possess sufficient energy to escape the cluster potential (Vandenberg & Faulkner 1977). This, however, has been called into question by observations of giant stars with wind velocities exceeding the typical cluster escape velocity (Smith et al. 2004). What is more, energy injection from the usually neglected, although vast, main sequence stellar population could play a decisive role in mediating mass retention in these systems (Smith 1999).

Motivated by this line of reasoning, we present a systematic investigation of the impact of outflows emanating from both evolved and non-evolved stellar members on the intracluster gas evolution. To aid in our interpretation of the data, we compare observational constraints with the results of hydrodynamical simulations that include radiative cooling as well as mass and energy injection from the cluster members, which we derive using stellar evolution models. It is shown that the observational constraints of intracluster gas can be successfully explained in models where the expulsion of evolved stellar ejecta is caused by the efficient thermalization of the energy emanating from the main sequence stellar population. In globular clusters with stringent gas density constraints, such as 47 Tucanae, M15, NGC 6440, and NGC 6752, we argue that energy output from the main sequence stellar population alone is capable of efficiently clearing out the evolved stellar ejecta. Since the majority of clusters with stringent gas content constraints host millisecond pulsars, we extend our calculations to include the energy injection supplied by their winds. The detection of ionized gas in 47 Tucanae, in particular, allows us to place strict limits on the pulsar wind thermalization efficiency within these systems.

2. MODELING GAS IN GLOBULAR CLUSTERS

We begin with a simple calculation to estimate the intracluster gas density (Pfahl & Rappaport 2001), considering a cluster comprised of $N = 10^6 N_6$ stars with masses of $0.9 M_\odot$ at the main sequence turn-off. The ratio of evolved stars to the total number of stars within the cluster is roughly $N_{\text{to}}/N \approx 0.01$, resulting in an average separation of

$$r_\perp = 6.4 \times 10^{17} \left(\frac{N_{\text{to}}}{10^2} \right)^{-1/3} \left(\frac{r_h}{1 \text{pc}} \right) \text{ cm}, \quad (1)$$

where r_h represents the cluster half-light radius. Making the assumption that the wind from each evolved stellar member extends only to its nearest neighbors, a lower limit on the cluster gas density may be obtained. Under this assumption, the cluster gas density is found to be

$$n_\perp = 0.1 \left(\frac{N_{\text{to}}}{10^2} \right)^{2/3} \left(\frac{r_h}{1 \text{pc}} \right)^{-2} \left(\frac{v_{\text{w,to}}}{70 \text{ km s}^{-1}} \right)^{-1} \left(\frac{\dot{M}_{\text{w,to}}}{10^{-7} M_\odot \text{ yr}^{-1}} \right) \text{ cm}^{-3}, \quad (2)$$

where $\dot{M}_{\text{w,to}}$ and $v_{\text{w,to}}$ correspond to the mass loss rate and wind velocity of the evolved stellar members (Section 3.2 contains a more detailed description of stellar evolution models). This lower limit may then be contrasted with a

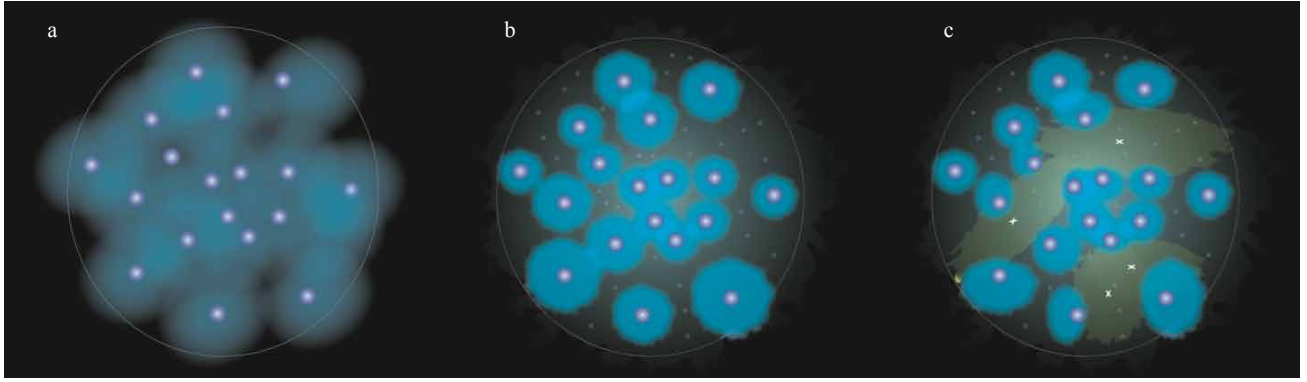


FIG. 1.— Diagram illustrating the different mass and energy contributions arising from main sequence stars, evolved stars and pulsar winds. If evolved stars dominate the mass and energy injection, a lower limit on the gas density can be calculated by assuming that their emanating winds extend only to their closest neighbors (panel *a*). While the evolved stellar members are expected to dominate the mass injection, despite comprising a small subset of the stellar cluster population, the energy injection is likely to be dominated by the more abundant main sequence stars (panel *b*) and, in some clusters, by millisecond pulsar winds (panel *c*). A significant amount of energy injection could prevent the winds from the evolved stellar members from effectively expanding between closest neighbors, resulting in lower gas content. This is illustrated in panels *b* and *c* when the energy injection is dominated by main sequence stars and pulsar winds, respectively.

second case, where evolved stellar winds extend to fill the volume of the entire cluster. The density for this second scenario is found to be

$$n_h = 1.5 \left(\frac{N_{\text{to}}}{10^2} \right) \left(\frac{r_h}{1 \text{ pc}} \right)^{-2} \left(\frac{v_{w,\text{to}}}{70 \text{ km s}^{-1}} \right)^{-1} \left(\frac{\dot{M}_{w,\text{to}}}{10^{-7} M_\odot \text{ yr}^{-1}} \right) \text{ cm}^{-3}. \quad (3)$$

In fact, we suspect that the gas density may exceed n_h if $v_{w,\text{to}} \lesssim \sigma$, where σ is the velocity dispersion of the cluster, when the gravitational effects of the cluster are taken into consideration (Pflamm-Altenburg & Kroupa 2009). On the other hand, if significant energy injection takes place within the cluster, the gas density is expected to be lower than the lower gas density limit n_\perp . The impact of energy injection on the intracluster gas content is presented in Figure 1 for two illustrative cases: the emanation of hot winds from an abundant main sequence population alone (panel *b*) and from the combined effort of the main sequence stellar winds and millisecond pulsar winds (panel *c*). Much of our effort in this paper will be dedicated to determining the state of the intracluster gas in various globular clusters, and describing how the expected energy injection from main sequence and millisecond pulsar populations may affect mass retention in these systems.

3. NUMERICAL METHODS AND INITIAL SETUP

3.1. Hydrodynamics

Our investigation of evolved stellar ejecta retention within globular clusters is mediated by hydrodynamical simulations incorporating energy and mass injection. For the purpose of simplicity, spherical symmetry is assumed (Quataert 2004; Hueyotl-Zahuantitla et al. 2010). FLASH, a parallel, adaptive-mesh hydrodynamical code (Fryxell et al. 2000), is employed to solve the hydrodynamical equations in one-dimension. Within the cluster, emanating winds from the dense stellar population and millisecond pulsars, when present, are assumed to shock and thermalize and, as such, the mass and energy contributions are implemented as source terms in the hydrodynamical equations. In spherical symmetry, the hydrodynamical equations may be written in the following form:

$$\frac{\partial \rho}{\partial t} + \frac{1}{r^2} \frac{\partial}{\partial r} (\rho u r^2) = q_{m,\star}(r, t) \quad (4)$$

$$\frac{\partial u}{\partial t} + u \frac{\partial u}{\partial r} + \frac{1}{\rho} \frac{\partial P}{\partial r} = -\frac{d\Phi_g}{dr} - q_{m,\star}(r, t)u \quad (5)$$

$$\frac{\partial \varepsilon}{\partial t} + \frac{1}{r^2} \frac{\partial}{\partial r} (\varepsilon u r^2) + P \frac{\partial u}{\partial r} = q_{\varepsilon,\star}(r, t) + q_{\varepsilon,\Omega}(r, t) - Q(r), \quad (6)$$

where $P = P(r)$, $\rho = \rho(r)$, $u = u(r)$ and $\varepsilon = \varepsilon(r)$ correspond to the gas pressure, density, radial velocity and internal energy density, respectively (Holzer & Axford 1970; Hueyotl-Zahuantitla et al. 2010). $Q(r) = n_i(r)n_e(r)\Lambda(T, Z)$ is the cooling rate for a gas consisting of ion and electron number densities, $n_i(r)$ and $n_e(r)$, and the cooling function for gas of temperature T with metallicity Z is represented by $\Lambda(T, Z)$. Cooling functions are taken from Gnat & Sternberg (2007) for $T > 10^4$ K and from Dalgarno & McCray (1972) for $10 \leq T \leq 10^4$ K.

In equations (4)-(6), the terms $q_{m,\star}(r, t)$ and $q_{\varepsilon,\star}(r, t)$ respectively represent the rates of mass and energy injection produced by the evolved stellar ejecta at a time t in a cluster's history. Stellar winds dominate cluster mass injection, and, as a result, the hydrodynamical influence of the millisecond pulsars is restricted to the energy injection term:

$q_{\varepsilon,\Omega}(r,t)$. Given N stars, each with an average mass loss rate (at a particular evolutionary time t) of $\langle \dot{M}(t) \rangle$ and a wind energy injection rate $\frac{1}{2}\langle \dot{M}(t) \rangle \langle v_w(t)^2 \rangle$, we find a total mass loss of $\dot{M}(t)_{w,\text{total}} = N\langle \dot{M}(t) \rangle = \int 4\pi r^2 q_m(r,t) dr$ and a total wind energy injection of $\dot{E}(t)_{w,\star,\text{total}} = \frac{1}{2}N\langle \dot{M}(t) \rangle \langle v_w(t)^2 \rangle = \int 4\pi r^2 q_{\varepsilon,\star}(r,t) dr$, where $q_{\varepsilon,\star}(r,t) = \frac{1}{2}q_m(r,t)\langle v_w(t)^2 \rangle$. In order to preserve simplicity, we have ignored the effects of mass segregation. In addition, we assume $q_m(r,t) \propto n_\star(r)$, such that $q_m(r,t) = A(t)r^{-2}\frac{d}{dr}\left(r^2\frac{d\Phi_g}{dr}\right)$, where $A(t) = \langle \dot{M}(t) \rangle / (4\pi G \langle M_\star \rangle)$ and $\langle M_\star \rangle$ corresponds to the average mass of a star.

The stellar cluster gravitational potentials are simulated with a Plummer model, which takes the form

$$\Phi_g = -\frac{GM_c}{[r^2 + r_c^2(\sigma_v)]^{1/2}} \quad (7)$$

for a total cluster of mass M_c with velocity dispersion $\sigma_v = (3^{3/4}/\sqrt{2})^{-1}\sqrt{GM_c/r_c}$ (Brüns et al. 2009; Pflamm-Altenburg & Kroupa 2009). It should be noted that while the shape of the potential can impact the radial distribution of gas within the core (Naiman et al. 2011), the total amount of gas accumulated within the cluster is relatively unaffected by the shape of the potential. In addition, to account for the gas dynamics under the influence of Φ_g , the self gravity of the gas is computed using FLASH's multipole module. The resolution is fixed to 6400 radial cells for each model. The core radius, r_c , sets the resolution within the computational domain, ensuring that we adequately resolve the core and setting a cluster potential of effectively zero at the outer boundary.

3.2. Stellar Evolution

Our simulations are highly dependent upon two key parameters: the time dependent average stellar mass loss rate and stellar wind velocity. The average stellar mass loss rate and stellar wind velocity then directly determine the mass and energy injection rates, $q_{m,\star}$ and $q_{\varepsilon,\star}$. These rates must encompass the average mass loss properties of the stellar population as a whole, since we are employing spherically symmetric simulations.

3.2.1. The Turn Off Approximation

To approximate the total mass loss and mean thermal velocities of the colliding winds within the cluster, we employ the formalism developed by Pooley & Rappaport (2006). In the relations

$$\langle v_{w,\text{to}}^2 \rangle \approx \frac{2\Delta E_K}{\Delta M} \quad (8)$$

and

$$\langle \dot{M}_{\text{to}} \rangle \approx \frac{\Delta M}{\Delta t}, \quad (9)$$

the integrated kinetic energy of the stellar winds and mass loss by the stellar population's turn off stars has been used as a proxy for the average values. The kinetic energy of the winds is given by $\Delta E_K = \frac{1}{2}\int_{t_0}^{t_1}\dot{M}_{\text{to}}v_{w,\text{to}}^2 dt$ and $\Delta M = \int_{t_0}^{t_1}\dot{M}_{\text{to}} dt$ denotes the mass loss input rate integrated over the lifetime of the turn-off stars, $\Delta t = t_1 - t_0$, where t_0 is the zero age main sequence (ZAMS) and t_1 is the onset of the white dwarf stage. While this approximation provides a reasonable estimate for the overall supply of wind mass and energy to the cluster, it fails to capture realistic stellar wind variability, which is currently not well constrained (Marigo 2012; Wood et al. 2005; Cohen 2011).

3.2.2. The Population Averaged Approximation

Neglected in the formalism outline above are the effects from the addition of mass and kinetic energy input from stars with $M_\star < M_{\text{to}}$. These effects may be included by convolving the given definitions of the average mass loss rate and stellar wind velocity with an initial mass function (IMF) and a star formation history. Following the logic of Kroupa et al. (2013), the average number of stars in a mass interval $[M_\star, M_\star + dM_\star]$ evolving between a span of time $[t, t + dt]$ is given by the relation $dN = \zeta(M_\star, t)N_\star b(t)dM_\star dt$ where $\zeta(M_\star, t)$ denotes the IMF, assumed to be accurately described by the Kroupa (2001) IMF, the normalized star formation history is given by $b(t)$, and N_\star is the total number of stars within the cluster. For a non-evolving IMF, $\zeta(M_\star, t) = \zeta(M_\star)$, comprised of a mass distribution extending from masses M_L to M_H , the normalized star formation history is given by $1/t_{\text{age}}(M_L)\int_0^{t_{\text{age}}(M_L)} b(t)dt = 1$, where $t_{\text{age}}(M_\star)$ denotes the lifetime of a star of a given M_\star and $b(t) = \delta(t - t_0)$ for a population of coeval stars forming at t_0 .

The average mass $\langle \Delta M(t_i) \rangle$ and kinetic energy $\langle \Delta E_K(t_i) \rangle$ injection within the cluster at a time t_i , by a population of stars of $M_\star \in [M_L, M_H]$ whose birth rate is regulated by $b(t)$, may then be formalized as

$$\langle \Delta M(t_i) \rangle = \int_{t_0}^{t_i} b(t) \int_{M_L}^{M_H} \zeta(M_\star) \dot{M}(M_\star, t) dM_\star dt \quad (10)$$

and

$$\langle \Delta E_K(t_i) \rangle = \frac{1}{2} \int_{t_0}^{t_i} b(t) \int_{M_L}^{M_H} \zeta(M_\star) \dot{M}(M_\star, t) v_w^2(M_\star, t) dM_\star dt, \quad (11)$$

respectively. Stars with lifetimes $t_{\text{age}}(M_\star) < t_i$ abandon the stellar population and are not included in the averaging. For any given time $t_i = t_{\text{to}}$, $M_{\text{H}} = M_{\text{to}}$, permitting us to split these equations into their corresponding turn off and main sequence components. These are given by

$$\langle \Delta M(t_i) \rangle = \langle \Delta M_{\text{to}} \rangle + f_{\text{ms}} \langle \Delta M_{\text{ms}} \rangle = \zeta(M_{\text{to}}) \int_{t_0}^{t_i} b(t) \dot{M}(M_{\text{to}}, t) dt + f_{\text{ms}} \int_{t_0}^{t_i} b(t) \int_{M_{\text{L}}}^{M_{\text{H}} < M_{\text{to}}} \zeta(M_\star) \dot{M}(M_\star, t) dM_\star dt \quad (12)$$

and

$$\begin{aligned} \langle \Delta E_K(t_i) \rangle &= \langle \Delta E_{K,\text{to}} \rangle + f_{\text{ms}} \langle \Delta E_{K,\text{ms}} \rangle \\ &= \frac{1}{2} \zeta(M_{\text{to}}) \int_{t_0}^{t_i} b(t) \dot{M}(M_{\text{to}}, t) v_w^2(M_{\text{to}}, t) dt + \frac{f_{\text{MS}}}{2} \int_{t_0}^{t_i} b(t) \int_{M_{\text{L}}}^{M_{\text{H}} < M_{\text{to}}} \zeta(M_\star) \dot{M}(M_\star, t) v_w^2(M_\star, t) dM_\star dt, \end{aligned} \quad (13)$$

where the fraction of the main sequence stellar winds that is effectively thermalized and mixed within the cluster environment is denoted by f_{ms} . After leaving the main sequence branch, the majority of a star's mass is lost and, as such, we approximate $\langle \Delta M(t_i) \rangle \approx \langle \Delta M_{\text{to}} \rangle$. As a result, equations (8) and (9), representing the average stellar wind velocity and average stellar mass loss rate, may then be cast into the more general form

$$\begin{aligned} \langle v_w^2(t_i) \rangle &= \frac{2 \langle \Delta E_K(t_i) \rangle}{\langle \Delta M(t_i) \rangle} \approx \frac{2(\langle \Delta E_{K,\text{to}} \rangle + f_{\text{ms}} \langle \Delta E_{K,\text{ms}} \rangle)}{\langle \Delta M(t_{\text{to}}) \rangle} \\ &= \frac{\int_{t_0}^{t_i} b(t) \dot{M}(M_{\text{to}}, t) v_w^2(M_{\text{to}}, t) dt}{\int_{t_0}^{t_i} b(t) \dot{M}(M_{\text{to}}, t) dt} + f_{\text{ms}} \frac{\int_{t_0}^{t_i} b(t) \int_{M_{\text{L}}}^{M_{\text{H}} < M_{\text{to}}} \zeta(M_\star) \dot{M}(M_\star, t) v_w^2(M_\star, t) dM_\star dt}{\zeta(M_{\text{to}}) \int_{t_0}^{t_i} b(t) \dot{M}(M_{\text{to}}, t) dt}. \end{aligned} \quad (14)$$

and

$$\langle \dot{M}(t_i) \rangle \approx \frac{\langle \Delta M_{\text{to}} \rangle}{t_i} = \frac{1}{t_i} \zeta(M_{\text{to}}) \int_{t_0}^{t_i} b(t) \dot{M}(M_{\text{to}}, t) dt, \quad (15)$$

for a given stellar population lifetime t_i .

Individual mass loss rates $\dot{M}(M_\star, t)$ and wind velocities $v_w(M_\star, t)$ are calculated with MESA stellar evolution models (Paxton et al. 2011). MESA follows the evolution of a grid of stellar models with $M_\star = 0.6 M_\odot - 8 M_\odot$ from ZAMS to the white dwarf stage. The wind velocity is approximated to be equal to the escape velocity, accurate within a factor of a few across a wide range of masses and life stages (Abbott 1978; Evans et al. 2004; Schaerer et al. 1996; Nyman et al. 1992; Vassiliadis & Wood 1993; Loup et al. 1993; Dupree & Reimers 1987; Debes 2006; Badalyan & Livshits 1992). MESA uses the Reimers (1975) prescription, given by $\dot{M}_R = 4 \times 10^{-13} \eta_R (M/M_\odot)^{-1} (L/L_\odot) (R/R_\odot) M_\odot \text{yr}^{-1}$, where $\eta_R = 1.0$, to estimate the stellar mass loss over the RGB branch and main sequence lifetime. As illustrated in Figure 2, this prescription provides a reasonable estimate for the stellar mass loss rates of low mass main sequence stars, which can be also approximated by $\dot{M}_{\text{ms}} \approx 10^{-12} (M/M_\odot)^3 M_\odot \text{yr}^{-1}$. Also shown in Figure 2 are the values expected for the injected luminosity and average wind velocity per star as a function of the stellar population's turn-off mass and metallicity. The different contributions to the mass and energy arising from the evolved stars alone (M_{to}) as well as from both evolved stars and main sequence stars together (M_{ms}) are compared in the figure. To highlight their importance, we have assumed that the main sequence stellar winds are effectively thermalized and mixed within the cluster (i.e., $f_{\text{ms}} = 1$). While there is observational evidence that metallicity does not strongly impact the mass loss rate of main sequence stars (McDonald & van Loon 2007; Sloan et al. 2008), stellar wind velocities are found to scale with metallicity (Marshall et al. 2004). This explains the Z -dependence observed in Figure 2.

4. THE ROLE OF STELLAR WIND HEATING

Within a cluster, main sequence stellar members are far more prevalent than evolved stars and, as a result, their contribution to the heating of the intracluster environment should be taken into account (Smith 1999). Employing spherically symmetric one-dimensional hydrodynamical simulations, we investigate the state of the intracluster gas, whose evolution is mediated by energy and mass injection by both the main sequence and evolved stellar populations. The injection of energy by a much less abundant, yet more individually energetic, population of millisecond pulsars will not be examined until Section 5. The thermalization and mixing of the main sequence stellar winds is regulated in our simulations by the efficiency f_{ms} , with a range of $[0, 1]$, where 0 represents a complete lack of thermalization and mixing, while 1 denotes a perfectly thermalized, mixed wind contribution from the main sequence stars. Modeling the cluster masses, core radii, and velocity dispersions for specific clusters, we are able to compare our computational results to density constraints determined by observation.

The simulation results for cluster parameters set to match that of the Galactic globular clusters M15 are shown in Figure 3. A cluster mass of $M_c = 4.4 \times 10^5 M_\odot$ (McNamara et al. 2004) and a cluster velocity dispersion of $\sigma_v = 28 \text{ km s}^{-1}$ (Harris 1996) was employed. Figure 3 displays the free electron density, neutral hydrogen density, temperature, and wind flow velocity profiles, where dashed lines indicate the electron and neutral hydrogen upper limits from Freire et al. (2001b) and Anderson (1993), respectively. Here, electron and neutral hydrogen fractions are determined with

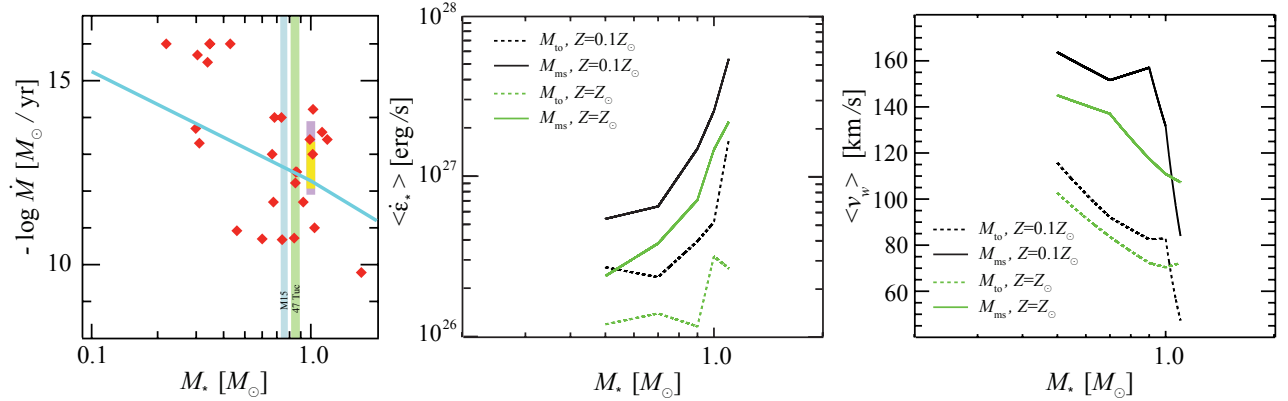


FIG. 2.— The relationship between stellar mass loss rates and energy injection in globular clusters as a function of the population’s turn-off mass. *Left Panel:* The mass loss rate estimates along the main sequence are plotted as a function of the turn-off mass of the stellar population. The *light blue* line shows our model inputs from MESA, while the *diamond* symbols show a compilation of observed mass loss rates (Crammer & Saar 2011; de Jager et al. 1988; Searle et al. 2008; Waters et al. 1987; Debes 2006; Badalyan & Livshits 1992; Morin et al. 2008). The *yellow* rectangular region shows the estimated changes in the mass loss rate of the Sun over the past 1-5 Gyrs while the *purple* rectangular region illustrates the variability in the mass loss rate as derived by the solar X-ray activity (Wood et al. 2005; Cohen 2011). It is important to note that not only do different stars demonstrate variability in mass loss rates, but this rate can also vary in individual stars themselves. This motivates the need for a normalized mass loss prescription, as it would not be possible to accurately model the variability in our cluster sample. The *blue* and *green* vertical shaded regions shows the approximate age range estimated for M15 and 47 Tucanae, respectively. *Middle Panel:* The injected luminosities per star are plotted as a function of the stellar population’s turn-off mass and metallicity. The energy injection has been calculated using the contribution of the turn-off mass stars alone (M_{to}) as well as adding the main sequence stellar contribution (M_{ms}) for which we have assumed perfect thermalization and mixing, $f_{\text{ms}} = 1$. *Right Panel:* The corresponding average stellar wind velocity per star is shown as a function of the stellar population’s turn-off mass and metallicity. In both *middle* and *right* panels the *dotted green* lines represents stars with solar metallicity $Z = Z_{\odot}$ and the *dotted black* lines denote stars with $Z = Z_{\odot}/10$.

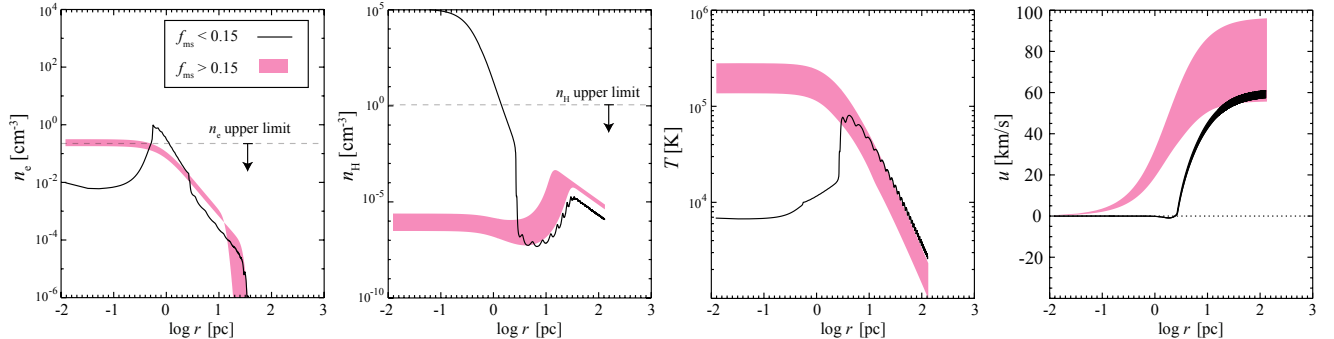


FIG. 3.— The state of the intracluster gas in the globular cluster M15 calculated using one-dimensional hydrodynamical simulations. Shown are the radial profiles of the electron n_e and neutral hydrogen n_{H} densities, the temperature T and the flow velocity u . The simulation assumes energy and mass injection is determined solely by main sequence and evolved stars. The main sequence stellar wind thermalization and mixing efficiency within the cluster is regulated by f_{ms} , whose range is $[0, 1]$. The dashed lines show the electron and neutral hydrogen upper limits from Freire et al. (2001b) and Anderson (1993), respectively. To model M15 we employ $M_c = 4.4 \times 10^5 M_{\odot}$ (McNamara et al. 2004) and $\sigma_v = 28 \text{ km s}^{-1}$ (Harris 1996). *Thin black* regions display models with $0 \lesssim f_{\text{ms}} < 0.15$, while *pink* regions depict models with $0.15 < f_{\text{ms}} \lesssim 1$. We find that only heating models with $f_{\text{ms}} > 0.15$ give results consistent with current observational constraints.

the assumption that the gas is in collisional equilibrium, and thus, the electron gas fraction is dependent upon the temperature alone. This amounts to solving for n_e and $n_{\text{H}} = n_{\text{H,tot}} + n_{\text{H}^+}$ in the collisional equilibrium equation $\alpha_{\text{rec}}(T)n_e n_{\text{H}^+} = C_{\text{ci}}(T)n_e n_{\text{H,tot}}$, where the recombination coefficient, $\alpha_{\text{rec}}(T)$, and the collisional ionization coefficient, $C_{\text{ci}}(T)$ are functions of the temperature of the gas, T (Hummer & Storey 1987; Padmanabhan 2000). The black region in this figure illustrates the parameter space for models where with $0 \lesssim f_{\text{ms}} < 0.15$, while the pink region depicts the parameter space where $0.15 < f_{\text{ms}} \lesssim 1$. The figure shows that only models with $f_{\text{ms}} > 0.15$ provide results that are consistent with observational constraints. Consequently, the low gas and dust levels observed in this cluster can be explained solely by the main sequence star heating if at least 15% of their emanating stellar winds are effectively thermalized and mixed with those of the evolved population.

Similarly, the simulation results for a cluster created to match the characteristics of 47 Tucanae are shown in Figure 4. We employed a cluster mass of $M_c = 6.4 \times 10^5 M_{\odot}$ (Marks & Kroupa 2010) and cluster velocity dispersion $\sigma_v = 27 \text{ km s}^{-1}$ (Bianchini et al. 2013). The resulting free electron density, neutral hydrogen density, temperature, and wind flow velocity profiles for the state of the intracluster gas in Galactic globular cluster 47 Tucanae are shown in Figure 4, where dashed lines represent the free electron and neutral hydrogen upper limits taken from Freire et al. (2001b) and Smith et al. (1990), respectively. The black region in this figure illustrates the parameter space for models

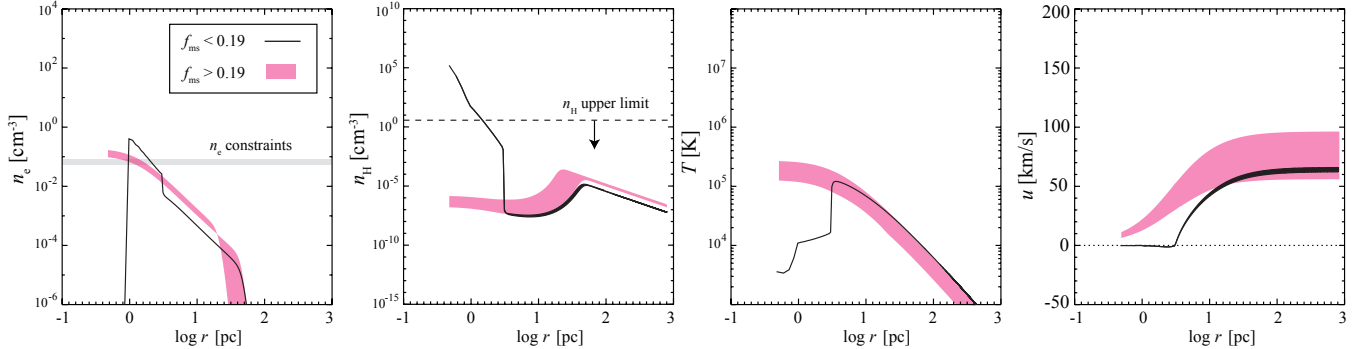


FIG. 4.— The state of the intracluster gas in the globular cluster 47 Tucanae calculated using one-dimensional hydrodynamical simulations. The radial profiles of the electron n_e and neutral hydrogen n_H densities, the temperature T and the flow velocity u assumes energy and mass injection is determined solely by main sequence and solved stars. The main sequence stellar wind thermalization and mixing efficiency within the cluster is regulated by f_{ms} , whose range is $[0, 1]$. Electron and neutral hydrogen upper limits are denoted by the dashed line and are taken from Freire et al. (2001b) and Smith et al. (1990), respectively. To model 47 Tucanae we employ $M_c = 6.4 \times 10^5 M_\odot$ (Marks & Kroupa 2010) and $\sigma_v = 27 \text{ km s}^{-1}$ (Bianchini et al. 2013). Thin black regions depict models with $0 \lesssim f_{\text{ms}} < 0.20$, while pink regions depict models with $0.20 < f_{\text{ms}} \lesssim 1$. We find that results are consistent with current observations only in heating models with $f_{\text{ms}} > 0.20$.

where with $0 \lesssim f_{\text{ms}} < 0.20$, while the pink region depicts the parameter space where $0.20 < f_{\text{ms}} \lesssim 1$. It is evident that only heating models with $f_{\text{ms}} > 0.20$ provide results that are consistent with current observational constraints. Thus, in order to explain the low gas and dust levels observed in this cluster solely by the heating supplied from main sequence members, a minimum of 20% of the stellar winds must be effectively thermalized and mixed into the cluster environment. Modeling 47 Tucanae is of significant importance, since after nearly half a century of searching, the first ever detection of ionized intracluster gas took place here. This constraint strongly limits the allowed values of f_{ms} .

In Figures 3 and 4 we have examined the free electron density n_e profiles, however we will be shifting our focus to the average density within the cluster's core \bar{n}_e as we compare the observationally allowed values of f_{ms} among different globular clusters. We have discussed the results of 47 Tucanae and M15, which happen to have similar velocity dispersions despite 47 Tucanae being about 1.45 times more massive. Comparing the four clusters in our sample we see that the velocity dispersion has a larger spread in values, while the masses are more similar. Additionally, Naiman et al. (2011) found that the cluster mass was less critical for gas retention when compared to the impact arising from changes in the velocity dispersion. Motivated by this, we have chosen to fix the cluster mass in an effort to systematically explore the effects of changing the velocity dispersion on the average free electron density \bar{n}_e and the average neutral hydrogen density \bar{n}_H .

Figure 5 displays the results of our effort to illustrate in more general terms how \bar{n}_e and \bar{n}_H change with velocity dispersion and f_{ms} for a cluster of fixed mass. As expected, we see that in general a larger cluster velocity dispersion results in an increase in density for both \bar{n}_e and \bar{n}_H . Figure 5 also indicates that the average free electron density is relatively independent of the stellar wind thermalization and mixing fraction, while the average neutral hydrogen density is more sensitive to changes in f_{ms} . At low velocity dispersions, the majority of the gas is easily removed from the cluster's potential regardless of the amount of main sequence heating, leading to the low electron and hydrogen number densities for $\sigma \lesssim 30 \text{ km s}^{-1}$. As the velocity dispersion increases, more material is funneled toward the central regions of the cluster, and for high enough dispersions, this gas effectively cools as it collects in the cluster's core. Because in this approximation the electron fraction is a function of temperature alone, the large central density enhancements which lead to large neutral hydrogen enhancements in the center result in relatively low electron fractions.

In Figure 6, we model the four clusters 47 Tucanae, M15, NGC 6440, and NGC 6752, where cluster masses and velocity dispersions are taken from Marks & Kroupa (2010) and Bianchini et al. (2013) for 47 Tucanae, McNamara et al. (2004) and Harris (1996) for M15, and Gnedin et al. (2002) for NGC 6440 and NGC 6752. With these parameters, we can explore the dependence of the free electron density and neutral hydrogen density, both averaged over the cluster core, on the stellar wind thermalization and mixing fraction. The density constraints shown in Figure 6 are from Anderson (1993), Freire et al. (2001b), Smith et al. (1990), Hui et al. (2009) and D'Amico et al. (2002). The density profiles from each of the four clusters are consistent with the strictest wind thermalization and mixing constraint, $f_{\text{ms}} \gtrsim 0.5$, determined by the detection of ionized gas in 47 Tucanae, and displayed as the shaded green region in Figure 6 (Freire et al. 2001b).

In summary, our models indicate that heating from the evolved and main sequence winds is essential in explaining the low density gas and dust observed in globular clusters and that a minimum of about 2/5 of the total stellar wind luminosity must effectively be thermalized and mixed into the cluster environment to provide an accurate description of current observational constraints. It is important to recognize that f_{ms} is the fraction of the total amount of energy injected by the main sequence stellar members, which has been calculated here using MESA. Consequently, the constraints we have derived on f_{ms} are relative in the sense that their definition depends on the exact value of the total injected energy, which is uncertain (Figure 2).

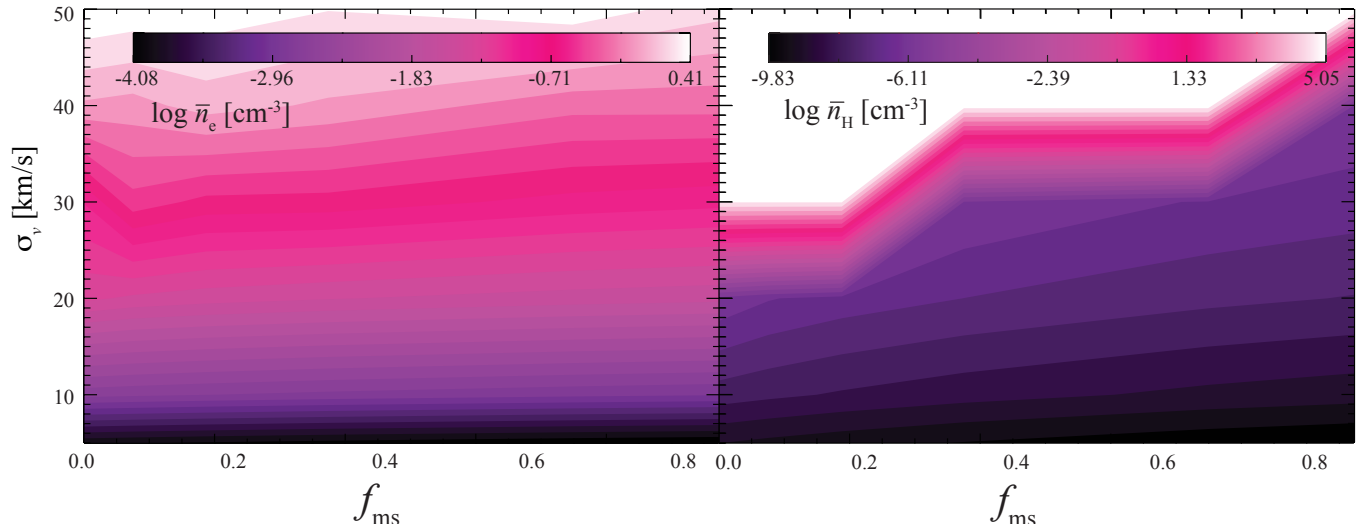


FIG. 5.— The relationship between a changing main sequence wind thermalization and mixing fraction f_{ms} and cluster velocity dispersion σ_v on the free electron density n_e (left panel) and n_{H} (right panel) averaged over the core. In both panels, the cluster mass was held at a constant value, $M_c = 5 \times 10^5 M_{\odot}$.

The role of pulsar heating in the evacuation of gas and dust in globular clusters was first discussed by Spiegel (1991). At that time the total number of detected millisecond pulsars residing in globular clusters was about two dozen. We now know of over 140 millisecond pulsars in 28 separate globular clusters (Freire 2013). In some of these clusters the population of millisecond pulsars is considerable. Globular cluster Terzan 5 is known to harbor 34 millisecond pulsars and 47 Tucanae contains 23 detected pulsars². In our hydrodynamical models, 47 Tucanae is used as a proxy to explore the physics of gas retention in clusters hosting a population of millisecond pulsars. This cluster was chosen because of the detection of ionized intracluster material (Freire et al. 2001b), which allows for strict constraints on the efficiency of pulsar heating to be placed.

The hydrodynamical influence of millisecond pulsars in our simulations is restricted to energy injection, $q_{\epsilon,\Omega}(r,t)$, as the stellar winds dominate the mass supply. For simplicity we assume that $q_{\epsilon,\Omega}(r) \propto n_p(r)$. As pulsar energy is predominately supplied as Poynting flux, the thermalization and mixing efficiency within the cluster core remains highly uncertain. In addition, also uncertain is the total amount of energy, \dot{E}_{Ω} , injected into the cluster. This uncertainty is largely due to unreliable timing solutions. For this reason, the total energy injected by the pulsars that is effectively thermalized and mixed into the cluster gas, \dot{E}_p , is treated as a free parameter and is parameterized here as $\dot{E}_p = f_p \dot{E}_{\text{ms}}$.

There are currently 16 millisecond pulsars within 47 Tucanae with known timing solutions. If we, for example, take the timing solutions at face value (Manchester et al. 1990, 1991; Robinson et al. 1995; Camilo et al. 2000; Edmonds et al. 2001; Freire et al. 2001a; Edmonds et al. 2002; Freire et al. 2003; Lorimer et al. 2003; Bogdanov et al. 2005), ignoring the likely possibility that they might be corrupted by cluster motions, we find a total spin-down luminosity of $\dot{E}_{\Omega} = 5.4 \times 10^{35} \text{ erg s}^{-1}$, which corresponds to $f_p = 24.4$ under the assumption that all of the spin down luminosity is effectively thermalized (i.e., $\dot{E}_p = \dot{E}_{\Omega}$). This would indicate an energy injection by the pulsar population that is 24.4 times larger than that added by the main sequence stellar winds. If, on the other hand, we assume that the luminosity distribution of millisecond pulsars residing in the cluster is well described by the luminosity function of Galactic field pulsars (Manchester et al. 2005), we obtain $\dot{E}_{\Omega} = 5 \times 10^{34} \text{ erg s}^{-1}$, which is an order of magnitude smaller than the total power estimated using 47 Tucanae’s pulsar timing parameters.

Figure 7 shows the free electron density, neutral hydrogen density, temperature, and flow velocity radial profiles for a cluster modeled after 47 Tucanae when heating from the millisecond pulsar population is included. In this figure, heating from the main sequence winds is not considered. Contrasting the resulting density profiles to the upper limits for 47 Tucanae, we can determine the critical level of heating required to account for the observed gas densities, assuming this evacuation mechanism worked in isolation. The pulsar heating fraction f_p is normalized here to the main sequence heating rate, where $f_p = 1$ corresponds to the total amount of heating from the millisecond pulsar winds being equal to that expected to be supplied by main sequence stars. Models with $f_p \approx 4.1 \times 10^{-2}$ are consistent with the free electron and neutral hydrogen density constraints. Other models shown in Figure 7 result in gas that is either too cold and dense (black line) or too hot and diffuse (red line) when compare to observations. We conclude that the pulsar energy injection needs to be much lower than the stellar wind contribution and, as a result, the currently poorly understood pulsar wind thermalization efficiency within the cluster’s core must be small. This can be clearly seen in Figure 8 by comparing the thermodynamical profiles generated by models that include pulsar heating with those that use main sequence stellar winds as the dominant energy injection mechanism. On the condition that the millisecond pulsars inject $5 \times 10^{34} \text{ erg s}^{-1}$, as inferred from the Galactic field population, the thermalization efficiency needs to

² <http://www.naic.edu/~pfreire/GCpsr.html>

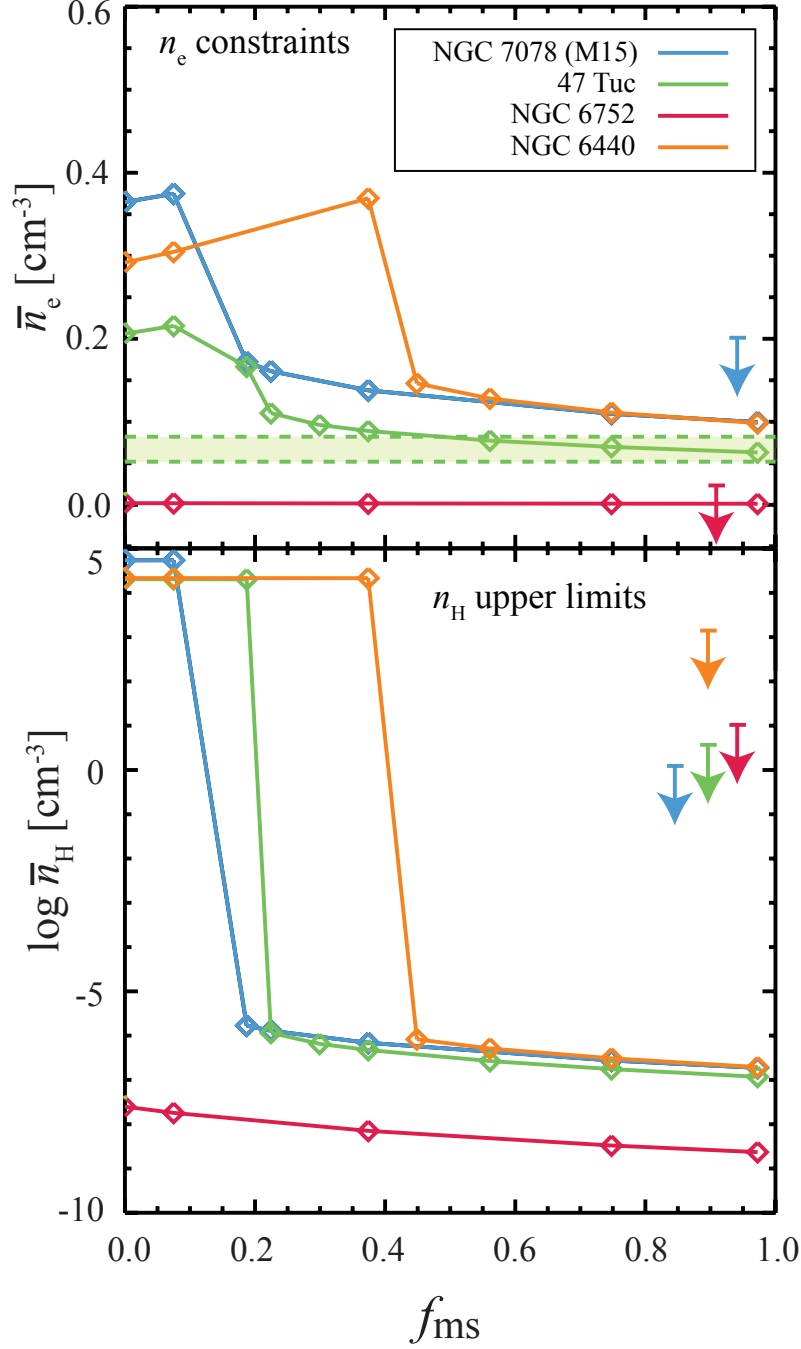


FIG. 6.— Free electron and neutral hydrogen densities, averaged over the cluster core, as a function of main sequence wind thermalization and mixing fraction for globular clusters 47 Tucanae, M15, NGC 6440, and NGC 6752. Upper limits are taken from Anderson (1993), Freire et al. (2001b), Smith et al. (1990), Hui et al. (2009), D’Amico et al. (2002). All of the profiles are consistent with the tightest stellar wind thermalization and mixing constraint of $f_{ms} \gtrsim 0.5$, provided by the 47 Tucanae electron density limits, and denoted in the figure by the shaded green region (Freire et al. 2001b). The cluster mass and velocity dispersion values are taken from Marks & Kroupa (2010) and Bianchini et al. (2013) for 47 Tucanae, McNamara et al. (2004) and Harris (1996) for M15, and Gnedin et al. (2002) for NGC 6440 and NGC 6752.

be $\lesssim 1.7\%$. If the thermalization efficiency within the cluster’s core was larger than this value, the observational constraints will be violated.

In Figure 9 we consider a more realistic scenario in which heating from both the main sequence stars and the millisecond pulsar populations is included. In this case, we search for models that produce thermodynamical profiles with average central electron and neutral hydrogen densities that are consistent with observational constraints when energy injection from both pulsars and stellar winds is taken into account. The blue-grey shaded regions in Figure 9 denote the parameter space that fall within the density constraints for 47 Tucanae. It is important to note the low levels of millisecond pulsar energy thermalization needed to explain the density limits even when the heating from the main sequence stellar winds is negligible. This is because of the overabundance of millisecond pulsars residing in the

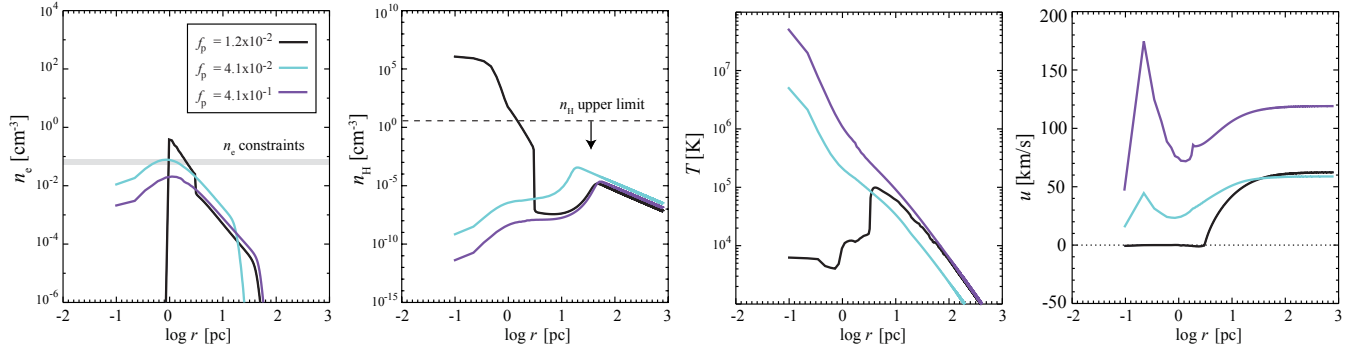


FIG. 7.— The state of the intracluster gas in the globular cluster 47 Tucanae, when only heating from the millisecond pulsar population is included. Shown are the radial profiles of the free electron density n_e , neutral hydrogen density n_H , temperature T , and flow velocity u , calculated using one-dimensional hydrodynamical simulations. Free electron and neutral hydrogen density limits are taken from Freire et al. (2001b) and Smith et al. (1990). The pulsar heating, represented by $\dot{E}_p = f_p \dot{E}_{ms}$, is normalized to the main sequence heating rate. Only models with $f_p \approx 4.1 \times 10^{-2}$ are consistent with the density constraints. The other models produce gas that is either too cool and dense (black line) or too hot and diffuse (red line) when compare with the observational limits.

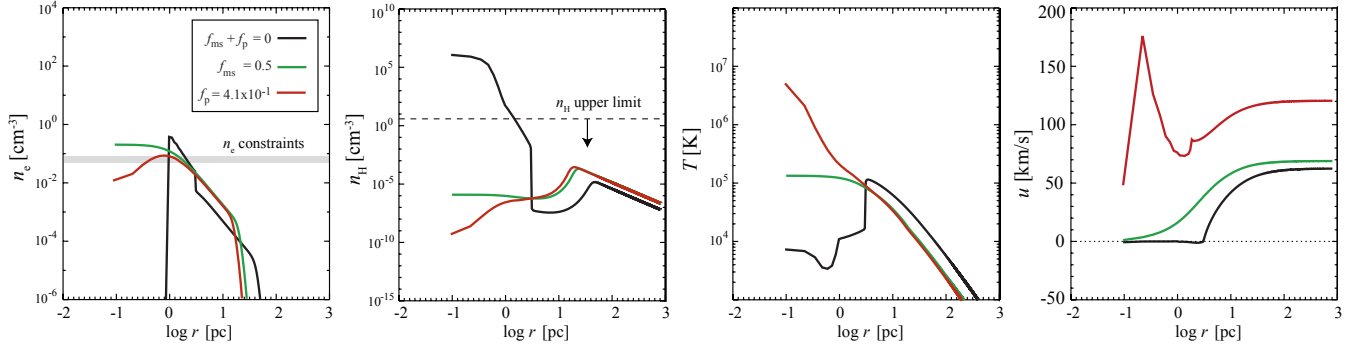


FIG. 8.— The state of the intracluster gas in the globular cluster 47 Tucanae as modified by heating from either the main sequence or the millisecond pulsar population. Shown are the radial profiles of the free electron density n_e , neutral hydrogen density n_H , temperature T , and flow velocity u , calculated using one-dimensional hydrodynamical simulations. Free electron and neutral hydrogen density limits are taken from Freire et al. (2001b) and Smith et al. (1990). The pulsar heating fractions, represented by f_p , are normalized to the main sequence heating rate.

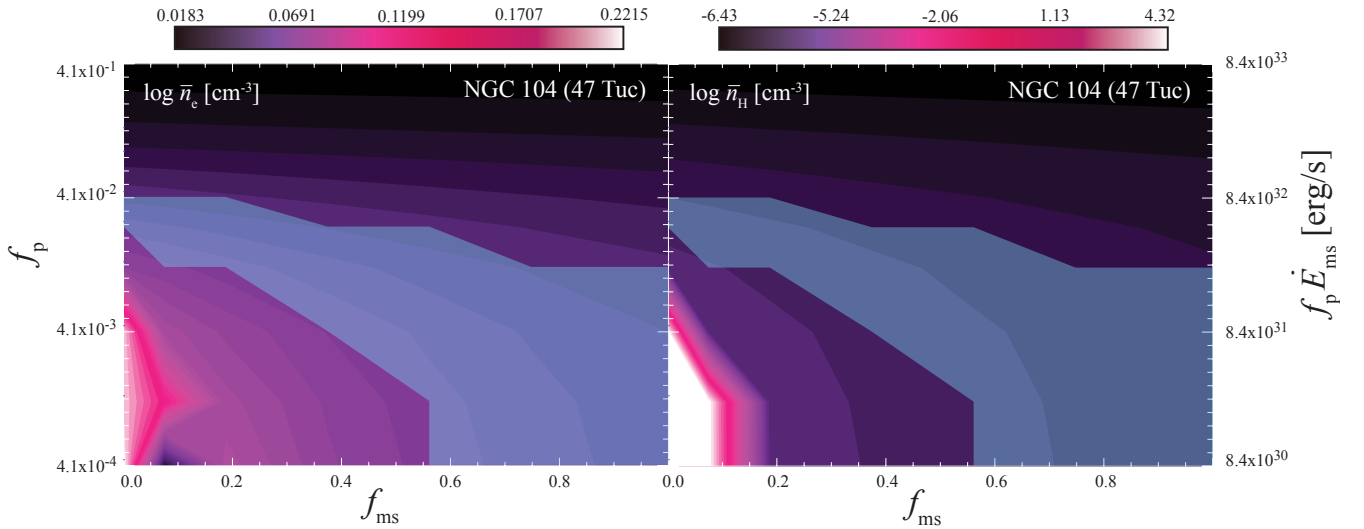


FIG. 9.— The state of the free electron density n_e and neutral hydrogen density n_H averaged over the core of the cluster as a function of millisecond pulsar heating and energy injection from the stellar winds for globular cluster 47 Tucanae. The blue-grey shaded denotes regions where our model is within the density constraints found by Freire et al. (2001b) and Smith et al. (1990). Note that our model places stringent constraints on the thermalization efficiency of pulsar winds in the core of 47 Tucanae.

core of 47 Tucanae, which helps prevent the intracluster gas from being effectively retained in the cluster. As such, we conclude that current observations place strong constraints on the ability of pulsar winds to effectively thermalize and mix within cluster's cores.

6. DISCUSSION

In this paper, we examine tenable gas evacuation mechanisms in an effort to account for the paucity of gas and dust in globular clusters. The tenuity of the intracluster medium is observed consistently from cluster to cluster and, as such, we aim to distinguish a mechanism that is universal in scope and not specific to variable cluster properties, such as, for example, UV heating from the HB stars (Vandenberg & Faulkner 1977) or stellar collisions (Umbreit et al. 2008). Energy injection by main sequence stellar members within a cluster is generally dismissed, primarily due to the fact that the energy contribution per star is low when compared to explosive processes, such as hydrogen rich novae (Scott & Durisen 1978; Moore & Bildsten 2011), and the heat input from individual evolved stars. We argue that the sheer abundance of the main sequence stellar members warrants this mechanism worthy of consideration. To this end, we construct one dimensional hydrodynamical models to study the properties of the gas in globular clusters with mass and energy injection provided by both the evolved and main sequence stellar populations. Choosing our initial conditions to match the cluster masses and core radii of globular clusters 47 Tucanae, M15, NGC 6440, and NGC 6752, we are able to compare our simulation results with observational density constraints. We find that a minimum of approximately 2/5 of the total stellar wind luminosity, which we calculate using MESA stellar evolution models, must be effectively thermalized and mixed into the cluster medium in order to generate results that are in agreement with current limits. We conclude that the energy output from the main sequence stellar population alone is capable of effectively sweeping out the evolved stellar ejecta in all the systems we have modeled. Specifically, we argue this result distinguishes a viable ubiquitous gas and dust evacuation mechanism for globular clusters. It is important to note that given current mass-loss uncertainties it is difficult to precisely quantify the fraction of effectively thermalized and mixed hot main sequence winds. However, it is clear that on the basis of commonly used mass-loss rate prescriptions, we expect energy injection from main sequence stars to play a vital role in regulating gas retention in globular clusters.

We extend our computational analysis to investigate the efficiency of pulsar wind feedback in a simulation modeled after the globular cluster 47 Tucanae, which is known to harbor 23 millisecond pulsars. The detection of intracluster ionized intracluster gas within 47 Tucanae allows for a detailed comparison between simulated results and the strict observational density constraints. The millisecond pulsar energy injection is known to be rather significant and, as such, we conclude that the pulsar wind thermalization efficiency must be extremely low in order to maintain the low density constraints for this cluster. Other clusters of interest in our analysis, M15, NGC 6440, and NGC 6752, are known to a host smaller populations of 8, 6, and 5 millisecond pulsars, respectively. While there is a high variability in the total pulsar energy injection per cluster, all observations indicate a tenuous intracluster medium. We argue that, when present, the millisecond pulsar population is rather ineffective at clearing gas within the cluster's core. The heat supplied by millisecond pulsars within a globular cluster is difficult to estimate, mainly due to the highly uncertain thermalization and mixing efficiency of the emanating Poynting flux within the core of the cluster. What needs to be demonstrated, perhaps by means of three dimensional, magneto-hydrodynamical simulations, is that pulsar outflows are not efficiently *poisoned* by the baryons emanating from the evolved stars by the time that they reach the edge of the cluster. We suspect, based on current observational constraints, that the pulsar wind energy is only efficiently thermalized at much larger radii. Observations of globular clusters with accompanying X-ray haloes support this idea (Mirabal 2010). In addition, it has been suggested by Hui et al. (2009) that while the luminous X-ray pulsar wind nebulae have been detected from pulsars in the Galaxy, there is no evidence of a contribution to the diffuse X-ray emission by pulsar wind nebulae within globular clusters. Searching for low and high energy diffuse emission within and around pulsar-hosting globular clusters could, in principle, help uncover the heating structures from these objects and provide a much clearer understanding of the underlying processes at work.

Our understanding of the intracluster medium has come a long way since observations revealed a dearth of gas within clusters over half a century ago, yet these gas-deficient systems continue to offer major puzzles and challenges. The modeling of mass retention in such dense stellar systems continues to be a formidable challenge to theorists and to computational techniques. The best prospects probably lie with performing three-dimensional (magneto)hydrodynamical simulations of the interaction of main sequence winds, evolved stellar winds and, when present in sizable numbers, pulsar winds. It is also a challenge for observers, in their quest for detecting the signatures of gas in extremely diffuse environments. Forthcoming space- and ground-based observations should provide the evidence necessary to unveil the detailed nature of the intracluster gas.

We acknowledge helpful discussions with C. Miller, C. Conroy, J. Strader, S. Ransom, M. Bailes, R. Parsons and J. Kalirai. Support was provided by the David and Lucile Packard Foundation and NSF grant AST-0847563. We thank the Aspen Center for Physics for its hospitality during the completion of this work.

REFERENCES

- ????
08. 1
Abbott, D. C. 1978, ApJ, 225, 893
Anderson, S. B. 1993, PhD thesis, California Institute of Technology, Pasadena.
Badalyan, O. G., & Livshits, M. A. 1992, AZh, 69, 138
Barmby, P., Boyer, M. L., Woodward, C. E., et al. 2009, AJ, 137, 207
Bianchini, P., Varri, A. L., Bertin, G., & Zocchi, A. 2013, ApJ, 772, 67
Birkinshaw, M., Ho, P. T. P., & Baud, B. 1983, A&A, 125, 271
Bode, M. F., & Evans, A. 2008, Classical Novae
Bogdanov, S., Grindlay, J. E., & van den Berg, M. 2005, ApJ, 630, 1029
Bowers, P. F., Kerr, F. J., Knapp, G. R., Gallagher, J. S., & Hunter, D. A. 1979, ApJ, 233, 553
Boyer, M. L., McDonald, I., Loon, J. T., et al. 2008, AJ, 135, 1395

- Boyer, M. L., Woodward, C. E., van Loon, J. T., et al. 2006, *AJ*, 132, 1415
- Brüns, R. C., Kroupa, P., & Fellhauer, M. 2009, *ApJ*, 702, 1268
- Camilo, F., Lorimer, D. R., Freire, P., Lyne, A. G., & Manchester, R. N. 2000, *ApJ*, 535, 975
- Cohen, N. L., & Malkan, M. A. 1979, *AJ*, 84, 74
- Cohen, O. 2011, *MNRAS*, 417, 2592
- Coleman, G. D., & Worden, S. P. 1977, *ApJ*, 218, 792
- Crammer, S. R., & Saar, S. H. 2011, *ApJ*, 741, 54
- Dalgarno, A., & McCray, R. A. 1972, *ARA&A*, 10, 375
- D'Amico, N., Possenti, A., Fici, L., et al. 2002, *ApJ*, 570, L89
- de Jager, C., Nieuwenhuijzen, H., & van der Hucht, K. A. 1988, *A&AS*, 72, 259
- Debes, J. H. 2006, *ApJ*, 652, 636
- Dickey, J. M., & Malkan, M. A. 1980, *AJ*, 85, 145
- Dupree, A. K., & Reimers, D. 1987, in *Astrophysics and Space Science Library*, Vol. 129, Exploring the Universe with the IUE Satellite, ed. Y. Kondo, 321–353
- Edmonds, P. D., Gilliland, R. L., Camilo, F., Heinke, C. O., & Grindlay, J. E. 2002, *ApJ*, 579, 741
- Edmonds, P. D., Gilliland, R. L., Heinke, C. O., Grindlay, J. E., & Camilo, F. 2001, *ApJ*, 557, L57
- Evans, A., Stickel, M., van Loon, J. T., et al. 2003, *A&A*, 408, L9
- Evans, C. J., Lennon, D. J., Trundle, C., Heap, S. R., & Lindler, D. J. 2004, *ApJ*, 607, 451
- Faulkner, D. J., & Freeman, K. C. 1977, *ApJ*, 211, 77
- Faulkner, D. J., Scott, T. R., Wood, P. R., & Wright, A. E. 1991, *ApJ*, 374, L45
- Frail, D. A., & Beasley, A. J. 1994, *A&A*, 290, 796
- Frank, J., & Gisler, G. 1976, *MNRAS*, 176, 533
- Freire, P. C., Camilo, F., Kramer, M., et al. 2003, *MNRAS*, 340, 1359
- Freire, P. C., Camilo, F., Lorimer, D. R., et al. 2001a, *MNRAS*, 326, 901
- Freire, P. C., Kramer, M., Lyne, A. G., et al. 2001b, *ApJ*, 557, L105
- Freire, P. C. C. 2013, in *IAU Symposium*, Vol. 291, IAU Symposium, 243–250
- Fryxell, B., Olson, K., Ricker, P., et al. 2000, *ApJS*, 131, 273
- Gnat, O., & Sternberg, A. 2007, *ApJS*, 168, 213
- Gnedin, O. Y., Zhao, H., Pringle, J. E., et al. 2002, *ApJ*, 568, L23
- Harris, W. E. 1996, *AJ*, 112, 1487
- Heiles, C., & Henry, R. C. 1966, *ApJ*, 146, 953
- Holzer, T. E., & Axford, W. I. 1970, *ARA&A*, 8, 31
- Hopwood, M. E. L., Evans, A., Penny, A., & Eyres, S. P. S. 1998, *MNRAS*, 301, L30
- Hopwood, M. E. L., Eyres, S. P. S., Evans, A., Penny, A., & Odenkirchen, M. 1999, *A&A*, 350, 49
- Hueyotl-Zahuantitla, F., Tenorio-Tagle, G., Wunsch, R., Silich, S., & Palouš, J. 2010, *ApJ*, 716, 324
- Hui, C. Y., Cheng, K. S., & Taam, R. E. 2009, *ApJ*, 700, 1233
- Hummer, D. G., & Storey, P. J. 1987, *MNRAS*, 224, 801
- Kerr, F. J., Bowers, P. F., & Knapp, G. R. 1976, in *Bulletin of the American Astronomical Society*, Vol. 8, Bulletin of the American Astronomical Society, 537
- Kerr, F. J., & Knapp, G. R. 1972, *AJ*, 77, 573
- Knapp, G. R., Gunn, J. E., Bowers, P. F., & Vasquez Poritz, J. F. 1996, *ApJ*, 462, 231
- Knapp, G. R., Gunn, J. E., & Connolly, A. J. 1995, *ApJ*, 448, 195
- Knapp, G. R., & Kerr, F. J. 1973, *AJ*, 78, 458
- Knapp, G. R., Rose, W. K., & Kerr, F. J. 1973, *ApJ*, 186, 831
- Kroupa, P. 2001, *MNRAS*, 322, 231
- Kroupa, P., Weidner, C., Pflamm-Altenburg, J., et al. 2013, *The Stellar and Sub-Stellar Initial Mass Function of Simple and Composite Populations*, ed. T. D. Oswalt & G. Gilmore, 115
- Leon, S., & Combes, F. 1996, *A&A*, 309, 123
- Lorimer, D. R., Camilo, F., Freire, P., et al. 2003, in *Astronomical Society of the Pacific Conference Series*, Vol. 302, Radio Pulsars, ed. M. Bailes, D. J. Nice, & S. E. Thorsett, 363
- Loup, C., Forveille, T., Omont, A., & Paul, J. F. 1993, *A&AS*, 99, 291
- Lynch, D. K., Bowers, P. F., & Whiteoak, J. B. 1989, *AJ*, 97, 1708
- Lynch, D. K., & Rossano, G. S. 1990, *AJ*, 100, 719
- Manchester, R. N., Hobbs, G. B., Teoh, A., & Hobbs, M. 2005, *VizieR Online Data Catalog*, 7245, 0
- Manchester, R. N., Lyne, A. G., Johnston, S., et al. 1990, *Nature*, 345, 598
- Manchester, R. N., Lyne, A. G., Robinson, C., Bailes, M., & D'Amico, N. 1991, *Nature*, 352, 219
- Marigo, P. 2012, in *IAU Symposium*, Vol. 283, IAU Symposium, 87–94
- Marks, M., & Kroupa, P. 2010, *MNRAS*, 406, 2000
- Marshall, J. R., van Loon, J. T., Matsuura, M., et al. 2004, *MNRAS*, 355, 1348
- McDonald, I., & van Loon, J. T. 2007, *A&A*, 476, 1261
- McNamara, B. J., Harrison, T. E., & Baumgardt, H. 2004, *ApJ*, 602, 264
- Mirabal, N. 2010, *MNRAS*, 402, 1391
- Moore, K., & Bildsten, L. 2011, *ApJ*, 728, 81
- Morin, J., Donati, J.-F., Petit, P., et al. 2008, *MNRAS*, 390, 567
- Naiman, J. P., Ramirez-Ruiz, E., & Lin, D. N. C. 2011, *ApJ*, 735, 25
- Nyman, L.-A., Booth, R. S., Carlstrom, U., et al. 1992, *A&AS*, 93, 121
- O'Brien, T. J., Bode, M. F., Porcas, R. W., et al. 2006, *Nature*, 442, 279
- Odenkirchen, M., Brosche, P., Geffert, M., & Tucholke, H.-J. 1997, *NA*, 2, 477
- Origlia, L., Ferraro, F. R., & Pecci, F. F. 1996, *MNRAS*, 280, 572
- Origlia, L., Gredel, R., Ferraro, F. R., & Fusi Pecci, F. 1997, *MNRAS*, 289, 948
- Padmanabhan, T. 2000, *Theoretical Astrophysics - Volume 1, Astrophysical Processes*
- Paxton, B., Bildsten, L., Dotter, A., et al. 2011, *ApJS*, 192, 3
- Pfahl, E., & Rappaport, S. 2001, *ApJ*, 550, 172
- Pflamm-Altenburg, J., & Kroupa, P. 2009, *MNRAS*, 397, 488
- Pooley, D., & Rappaport, S. 2006, *ApJ*, 644, L45
- Priestley, W., Ruffert, M., & Salaris, M. 2011, *MNRAS*, 411, 1935
- Quataert, E. 2004, *ApJ*, 613, 322
- Reimers, D. 1975, *Memoires of the Societe Royale des Sciences de Liege*, 8, 369
- Robinson, B. J. 1967, *Astrophys. Lett.*, 1, 21
- Robinson, C., Lyne, A. G., Manchester, R. N., et al. 1995, *MNRAS*, 274, 547
- Schaerer, D., de Koter, A., Schmutz, W., & Maeder, A. 1996, *A&A*, 310, 837
- Scott, E. H., & Durisen, R. H. 1978, *ApJ*, 222, 612
- Searle, S. C., Prinja, R. K., Massa, D., & Ryans, R. 2008, *A&A*, 481, 777
- Sloan, G. C., Kraemer, K. E., Wood, P. R., et al. 2008, *ApJ*, 686, 1056
- Smith, G. H. 1999, *PASP*, 111, 980
- Smith, G. H., Dupree, A. K., & Strader, J. 2004, *PASP*, 116, 819
- Smith, G. H., Wood, P. R., Faulkner, D. J., & Wright, A. E. 1990, *ApJ*, 353, 168
- Smith, G. H., Woodsworth, A. W., & Hesser, J. E. 1995, *MNRAS*, 273, 632
- Smith, M. G., Hesser, J. E., & Shawl, S. J. 1976, *ApJ*, 206, 66
- Spiegel, D. N. 1991, *Nature*, 352, 221
- Taylor, R. J., & Wood, P. R. 1975, *MNRAS*, 171, 467
- Troland, T. H., Hesser, J. E., & Heiles, C. 1978, *ApJ*, 219, 873
- Umbreit, S., Chatterjee, S., & Rasio, F. A. 2008, *ApJ*, 680, L113
- van Loon, J. T., Stanimirović, S., Evans, A., & Muller, E. 2006, *MNRAS*, 365, 1277
- van Loon, J. T., Stanimirović, S., Putman, M. E., et al. 2009, *MNRAS*, 396, 1096
- Vandenberg, D. A., & Faulkner, D. J. 1977, *ApJ*, 218, 415
- Vassiliadis, E., & Wood, P. R. 1993, *ApJ*, 413, 641
- Waters, L. B. F. M., Cote, J., & Lamers, H. J. G. L. M. 1987, *A&A*, 185, 206
- Wood, B. E., Müller, H.-R., Zank, G. P., Linsky, J. L., & Redfield, S. 2005, *ApJ*, 628, L143